International Journal of Pharmaceutics 421 (2011) 34–44

Contents lists available at SciVerse ScienceDirect

International Journal of Pharmaceutics

journal homepage: www.elsevier.com/locate/ijpharm

Investigation of microemulsion microstructures and their relationship to transdermal permeation of model drugs: Ketoprofen, lidocaine, and caffeine

Ji Zhang[a,b], Bozena Michniak-Kohn[a,b,*]

[a] Department of Pharmaceutics, Ernest Mario School of Pharmacy, Rutgers-The State University of New Jersey, Piscataway, NJ 08854, United States
[b] Laboratory for Drug Delivery & Center for Dermal Research, New Jersey Center for Biomaterials, Rutgers-The State University of New Jersey, Piscataway, NJ 08854, United States

ARTICLE INFO

Article history:
Received 1 June 2011
Received in revised form 6 September 2011
Accepted 15 September 2011
Available online 19 September 2011

Keywords:
Microemulsion microstructure
Transdermal
DSC
Water content
Oil content
Permeation enhancer

ABSTRACT

In this study, microemulsion microstructures, key formulation variables, and their relationship to drug transdermal permeation enhancement were investigated. A microemulsion system with high water soluble capacity was developed, using isopropyl myristate, Labrasol, and Cremophor EL as oil, surfactant, and co-surfactant, respectively. The microstructures of the microemulsions were characterized by a combination of techniques including electrical conductivity measurement (EC), differential scanning calorimetry (DSC), electro-analytical cyclic voltammetry (CV), dynamic light scattering (DLS). Three microemulsion formulations with the model drugs at water contents of 20%, 40%, and 70% representing the microstructures of W/O, Bi-continuous, and O/W were prepared along the water dilution line of oil to surfactant ratio of 1/9. Skin permeation of hydrophobic and hydrophilic model drugs, ketoprofen, lidocaine, and caffeine in the microemulsion formulations was studied using Franz-cells and dermatomed porcine skin. Permeation of all drugs from microemulsions was enhanced significantly compared with the control propylene glycol formulation. The drug permeation flux and the cumulative permeation amount after 24 h increased with water content in the microemulsions, thus correlated to the formulation microstructures of W/O, Bi-continuous, and O/W. The permeation of lipophilic drugs ketoprofen and lidocaine increased with water content in a more pronounced manner, which seemed to follow an exponential growth trend, while the permeation of hydrophilic drug caffeine appeared to increase linearly. Additionally, at the same water content, increasing oil content led to higher ketoprofen permeation.

1. Introduction

One of the major challenges for transdermal drug delivery is to increase the drug permeation through skin tissue by overcoming the skin barrier function from the stratum corneum. Many different approaches have been developed for this purpose including physical ones such as iontophoresis, sonophoresis, and micro-needles, and chemical or formulation ones such as permeation enhancers, co-solvents, liposomes, nano-particle suspensions, and microemulsions. Microemulsions are defined as single optically isotropic and thermodynamically stable dispersions of oil, water and surfactants with droplet sizes in the submicron range (Lee et al., 2003). They offer the advantages of high drug solubilizing capacity, long term stability, ease of preparation, and capability to enhance skin permeation for both hydrophobic and hydrophilic drugs (Heuschkel et al., 2008).

Microemulsion (ME) formulations can increase drug transdermal permeation, and this has been demonstrated for numerous drugs in past studies (Heuschkel et al., 2008; Neubert, 2011; Azeem et al., 2009; Kreilgaard et al., 2000; Kreilgaard, 2002; Sintov and Shapiro, 2004; Sintov and Botner, 2006; Sintov and Brandys-Sitton, 2006; Hua et al., 2004). So far, several hypotheses have been proposed on the mechanism for drug permeation enhancement, including increased drug solubility enabling a high concentration gradient toward skin, small droplet sizes and low viscosity of ME facilitating permeation, increased drug thermodynamic activity in the ME vehicle, and the disruption of SC lipid order by ME components, etc. However, there is a lack of systematic approaches in microemulsion formulation design and development mainly because the mechanism and factors controlling transdermal drug permeation enhancement are still not well understood.

Microemulsions exist in various microstructures including droplet-like and bi-continuous types. Since their drug delivery properties are related to the inner structure, there is a need to assign the correct state to the formulation. An appropriate characterization of ME microstructures is highly challenging due to their small particle sizes and fluctuation interfaces (Heuschkel et al., 2008). The combination of different characterization techniques is

* Corresponding author at: Department of Pharmaceutics, Ernest Mario School of Pharmacy, Rutgers-The State University of New Jersey, Piscataway, NJ 08854, United States. Tel.: +1 732 445 3589; fax: +1 732 445 5006.
E-mail address: michniak@biology.rutgers.edu (B. Michniak-Kohn).

0378-5173/$ – see front matter © 2011 Elsevier B.V. All rights reserved.
doi:10.1016/j.ijpharm.2011.09.014

required. Typically, the techniques used for microstructure assessment in drug transdermal delivery studies include viscosity test (Sintov and Shapiro, 2004; Djordjevic et al., 2004), surface tension test (Dong et al., 2011; Podlogar et al., 2005), electrical conductivity measurement (Alany et al., 2001; Djordjevic et al., 2005; Sintov and Shapiro, 2004; Mo and Li, 2007), DSC (Podlogar et al., 2004, 2005; Liu et al., 2009; Lopes et al., 2010), freeze-fracture transmission electron microscope (FF-TEM) (Alany et al., 2001; Dong et al., 2011), small angle X-ray scattering (SAXS) (Podlogar et al., 2005), and pulsed field gradient nuclear magnetic resonance (PFG-NMR) (Kreilgaard et al., 2000; Hua et al., 2004). Despite of studies in this area, there is still no clear understanding of microstructure relationship to ME formulation transdermal permeation potential. The reasons, in our view, are as follows: (1) the characterization of ME microstructures is not a straight forward task, and there is still lack of effective and simple methods to get unambiguous and accurate microstructure information, (2) there is a disconnect between studies on microstructures and those on drug transdermal permeation using ME formulations. The studies focused on microstructure examination were often confined in the structure probing aspect, and not extended to investigate further drug skin permeation. On the other hand, studies on transdermal permeation using ME formulations often only generated inadequate microstructure results or the ME systems in studies only had low water solubilizing capacity so that microstructure relationship to drug transdermal permeation could not be examined fully.

Therefore, the current study was conducted with multiple aims: (1) to explore the most effective techniques and their combination to characterize microemulsion microstructures; (2) to investigate microemulsion microstructure relationship to drug transdermal permeation enhancement for both lipophilic and hydrophilic drugs; (3) to investigate and identify key factors in ME that affect drug permeation potential; and (4) to explore permeation enhancement of microemulsions containing permeation enhancers, Azone and bromo-iminosulfurane (Song et al., 2005). In the study, a microemulsion system was developed, which had high water solubilizing capacity, thus allowing complete microstructure changes to be assessed at different water contents. Drug skin permeation was studied using Franz cell, dermatomed porcine skin and microemulsion formulations of specified microstructures containing model drugs ketoprofen, lidocaine, and caffeine.

2. Materials and methods

2.1. Materials

Isopropyl myristate (IPM) was purchased from Fisher Scientific (Fair Lawn, NJ). Cremophor EL was obtained from BASF (Ludwigshafen, Germany). Labrasol was obtained as a free sample from Gattefosse (St. Priest Cedex, France). Ketoprofen, lidocaine, caffeine, and ferrocene were purchased from Sigma (St. Louis, MO). Acetonitrile, methanol, and propylene glycol were purchased from Fisher Scientific (Fair Lawn, NJ). Water was distilled water that had been further purified by MilliQ A10 and Elix 10 systems.

2.2. Pseudo-ternary phase diagram construction

IPM was used as the oil phase (O), Labrasol was used as the surfactant (S), and Cremophor EL was used as co-surfactant (Co-S). First, the mixture of S and Co-S at the w/w ratio of 4:1 was prepared. Next, the mixture of O with S/Co-S was prepared at varying w/w ratios, e.g. 1:9, 2:8, 3:7, etc. Then, 1 g of the O/(S/Co-S) mixture of the certain ratio was titrated with water step by step, at each step, the H_2O/O/(S/Co-S) mixture was agitated by a vortex mixer to mix thoroughly, and the sample was checked under light versus a dark background. If the sample was an isotropic and clear solution, it was defined as a microemulsion; if the sample was cloudy or showed the phase separation, it was not a microemulsion. The observation, the corresponding O/(S/Co-S) ratio and the water content were recorded at each step of the titration. The boundary point between the microemulsion and the non-microemulsion was determined experimentally by measuring the mid-point between points of clear and cloudy samples. The microemulsion system pseudo-ternary phase diagram was constructed by labeling the recorded boundary points in a ternary plot. The accuracy of the boundary point determination is dependent on the water titration increment step, the smaller the step, the more accurate. However, the titration step cannot be infinitely small due to the limit of experimental conditions. In this study, the water titration increment step is about 3.3% (w/w). The mid-point method is more accurate than simply using the point of the cloudy sample. The technique was designed to obtain the region of ME existence to be as accurate as possible.

2.3. Microemulsion formulation preparation

The calculated amount of the model drug was weighed into a small glass vial, the exact amount of the O/(S/Co-S) mixture was added in, the compound was dissolved completely by the aid of sonication and vortex mixing. Then, the exact amount of water according to the design of the H_2O/(O/(S/Co-S)) w/w ratio was added in, and mixed well by vortex mixing.

Model drugs, ketoprofen, lidocaine, and caffeine were formulated in microemulsions with different water contents of 20%, 40% and 70% (w/w), representing the specific microstructures, W/O, Bi-continuous, and O/W, respectively. The drug loads (w/w %) in the formulations were set constant at 2.5%, 2.5%, and 1.0% for ketoprofen, lidocaine, and caffeine, respectively. The drug loading for caffeine was chosen to be lower due to its lower solubility in oils and surfactants. In order to characterize and examine caffeine-loaded W/O microemulsions, a reduced caffeine concentration was applied. Additional microemulsions with permeation enhancers, Azone and bromo-iminosulfurane (Br-IMSF), incorporated at 2% (w/w) were prepared. Propylene glycol (PG) formulations at the same drug loads were prepared and used as the controls. All above described formulations prepared were clear solutions at ambient temperature.

2.4. Microemulsion characterization

2.4.1. Dynamic light scattering (DLS)

The microemulsion internal phase apparent droplet diameter was measured using a DLS instrument, Zetasizer Nano Series Model Zen3600 (Malvern, Westborough, MA) at room temperature (at 25 °C ± 1 °C).

2.4.2. Refraction index

The microemulsion sample refraction index values were measured using a refractometer, ATAGO Model PAL-RI (ATAGO, Tokyo, Japan). The measurement was conducted at room temperature by adding 0.3 mL of the sample into the testing well.

2.4.3. Electrical conductivity (EC)

The microemulsion microstructure was assessed by EC tests. EC values of the sample were measured using an electric conductivity-meter, Oakton ECTestr 11+ (Ockton Instruments, Vernon Hills, IL). The conductivity-meter was calibrated using the standard solution of 1413 μS/cm (Ockton Instruments) before testing. Three grams of the oil–surfactant mixture of O/(S/Co-S) ratio 1/9 was titrated by the aqueous phase step by step, at each step, 1 mL of the sample was used for EC measurement at room temperature. The aqueous phase used was 0.9% (w/v) sodium chloride solution.

2.4.4. Electro analytical cyclic voltammetry (CV)

The microemulsion microstructure was evaluated by CV tests using a WaveNow Module cyclic voltammetry (CV) instrument with AfterMath software (Pine Research Instruments, Raleigh, NC). The method was based on and modified from that of Mo et al. (2000) and Mo and Li (2007). Ferrocene was used as the electro-chemical active probe compound in the experiment. Ferrocene is a very lipophilic compound and will dissolve mainly in oil phase when incorporated in microemulsion. Its diffusion coefficient would be mostly affected by the state of oil phase in microstructure, was measured by CV tests and used to deduce information of microemulsion microstructures. Ferrocene was initially dissolved in 10 g of oil–surfactant mixture of O/(S/Co-S) ratio 1/9 at the concentration of 0.5 mg/g, and diluted continuously by the aqueous phase (0.2 M KCl solution) while CV was conducted after each step of dilution at room temperature. CV conditions used were as follows: 2 segment run, start at −0.1 V, and end at 0.8 V with sweeping rates: 5, 10, 20, 40, 60, 80, and 100 mV/s. A glassy carbon electrode (surface area, 0.1963 cm^2) was used as the working electrode. A platinum wire and an AgCl/KCl electrode were used as the auxiliary electrode and the reference electrode, respectively. The anodic peak current, i_{pa} (A) at 25 °C will follow Randles–Sevcik equation (Eq. (1)),

$$i_{pa} = (2.687 \times 10^5) n^{3/2} v^{1/2} D^{1/2} AC \quad (1)$$

where n is the number of electron transferred in the electrochemical reaction, v is the sweeping rate (V/s), D is diffusion coefficient of ferrocene (cm^2/s), A is the surface area (cm^2) of the working electrode, and C is the concentration of electroactive probe, ferrocene (mole/cm^3). Therefore, based on the slope of the linear regression of i_{pa} vs. $v^{1/2}$ curve, diffusion coefficient of ferrocene, D, can be calculated.

2.4.5. Differential scanning calorimetry (DSC)

Microemulsions were tested using a TA Q100 DSC instrument (TA Instruments, New Castle, DE) for exploring the microstructures. Microemulsion sample (7–10 mg) was weighed accurately in an aluminum hermetic sample pan and sealed with the lid quickly to prevent the sample evaporation. DSC tests for blank ME samples were run at the following conditions: equilibrating at 25 °C for 1 min, cooling the sample at the ramp rate of 5 °C/min to −70 °C, isothermal for 0.5 min, heating the sample at the ramp rate of 5 °C/min to 30 °C. For model drug loaded ME formulation samples, DSC testing conditions are the same as those for blank ME samples except that the starting equilibration temperature is at 37 °C (for 10 min) to mimic the formulation sample temperature in the skin permeation experiment. The blank MEs were also tested by DSC at the starting temperature of 37 °C, and the data were similar to those obtained at 25 °C.

2.5. In vitro skin permeation experiment

Fresh porcine skin tissue from the abdomen was harvested from pigs (University of Medicine and Dentistry of New Jersey (UMDNJ), Dept. of Surgery, Newark, NJ). The tissue was carefully cleaned from fat and muscle, and then dermatomed to a thickness of around 500 μm. The dermatomed skin was then cut into pieces of about 14 mm × 14 mm that were stored at −80 °C until use. Typically, the storage time for the skin samples was less than 3 months. Franz diffusion cells were used for the in vitro permeation study with a receptor (5.1 mL) containing PBS buffer at 37 °C. The skin sample was mounted on the cell and was hydrated for 1 h prior to the experiment. Then, 150 μL of the microemulsion formulation or the control formulation was added to the donor. Propylene glycol with the same drug load was used as the control. The donors were sealed by Parafilm® immediately after the addition of the formulation to prevent water evaporation. At the time points of 0, 2, 16, 18, 20, 22, and 24 h, 300 μL of the receptor sample was taken and then replaced with the same amount of the fresh PBS buffer. The permeation samples were assayed immediately by HPLC. The drug steady-state permeation flux, J_s, is calculated based on data of time points from 16 to 24 h. The main purpose of the experiments was to measure the drug permeation steady-state flux, J_s, and the cumulative permeation amount, Q_{24}. The time points from 16 to 24 h were happened to be the right steady-state time period for the all three model drugs, therefore, the selection of sampling time points described in the above served the purpose. The preliminary experiments showed that the sampling time points in between 2 and 16 h (partly are in the lag period) would not be necessary for this work.

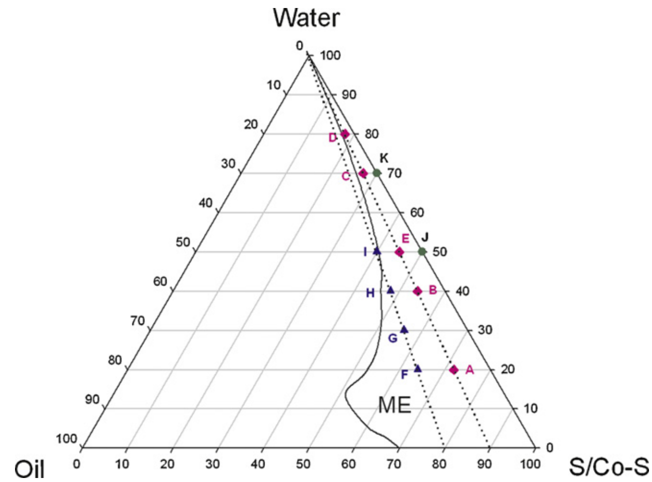

Fig. 1. A pseudo ternary phase diagram showing the system ME region and positions of ME and micelle formulations used in the permeation study. IPM, Labrasol, and Cremophor EL were used as oil, surfactant, and co-surfactant, respectively.

2.6. Model drug analyses

The permeation samples were analyzed using an Agilent 1100 HPLC equipped with a Luna C18(2) 5 μm 4.6 mm × 150 mm column (Phenomenex, Inc., Torrance, CA); mobile phases were (A) 0.1% H_3PO_4, and (B) acetonitrile. The run was conducted using an isocratic elution at A/B of 45/55, 80/20, and 85/15 for ketoprofen, lidocaine, and caffeine, respectively. The flow rate was 1 mL/min, the injection volume was 20 μL, and the UV detection wavelength was 258, 215, and 272 nm for ketoprofen, lidocaine, and caffeine, respectively. All assay methods were validated for linearity, inter- and intra-day variability as well as limit of detection.

2.7. Statistical analyses

The skin permeation results are reported as means ± S.D. Data was statistically analyzed using one-way ANOVA test followed by Fisher's post hoc test. Differences between formulations were considered significant when $P < 0.05$.

3. Results

3.1. Microemulsion characterization

3.1.1. Ternary phase diagram

The constructed pseudo ternary phase diagram is provided in Fig. 1. The ME region is identified, in which at the high surfactant

Table 1
Microemulsion apparent droplet size measured by DLS.

Microemulsion No.	Water content (w/w %)	Oil content (w/w %)	S/Co-S content (w/w %)	Drug load (w/w %)	Enhancer (w/w %)	Droplet size (nm)
1	20	8	72	None	None	177
2	30	7	63	None	None	86.8
3	40	6	54	None	None	50.0
4	50	5	45	None	None	34.2
5	60	4	36	None	None	22.8
6	70	3	27	None	None	17.3
7	80	2	18	None	None	14.3
8	70	3	27	None	Azone 2%	17.7
9	70	3	27	None	Br-IMSF 2%	22.2
10	70	3	27	Keto 1.0%	None	23.3
11	70	3	27	Keto 2.5%	None	42.3
12	80	2	18	Keto 2.5%	None	64.9
13	70	3	27	Caff 1.0%	None	18.4
14	70	3	27	Caff 1.0%	Azone 2%	21.1

Note: Keto, ketoprofen; Caff, ceffeine; Br-IMSF, bromo-iminosulfurane.

content area, a large amount of water can be solubilized without causing phase separation. For example, the oil–surfactant mixture at the O/(S/Co-S) ratio 1/9 can be diluted by water to higher than 95% (w/w) water content and the resulting sample still remained as a microemulsion. Therefore, along this water dilution line it is possible to study the complete course of microemulsion microstructure changes.

3.1.2. Refraction index

Along the water dilution line of O/(S/Co-S) ratio 1/9, microemulsions with different water content (Φ_W) were prepared and their refraction indexes (RI) were measured. The plot of RI vs. Φ_W shows a good linear correlation ($R^2 = 0.9996$), demonstrating microemulsion optically isotropic nature and high water solubilizing capacity of this ME system (Fig. 2).

3.1.3. Droplet size by dynamic light scattering

Microemulsions were prepared along the water dilution line of O/(S/Co-S) ratio 1:9. Their apparent droplet sizes assessed by DLS instrument are listed in Table 1. As can be seen the microemulsion apparent droplet size decreased significantly as water content increased, but the seemingly large change maybe an artifact. This is because the droplet size data in W/O region from DLS needs corrections from droplet–droplet interaction, vehicle viscosity, and continuous phase refraction index. For MEs in Bi-continuous region, the droplet size data are misleading because there are no real droplet entities in the region; however, the droplet size data in O/W region for the ME system is of meaningful value. For ketoprofen loaded MEs, at high water content (e.g. at Φ_W 70%), O/W droplet size increased significantly as ketoprofen concentration increased. In accordance with the solubility data presented in Table 2, indicating that ketoprofen is much more soluble in Labrasol than IPM, it is hypothesized that ketoprofen molecules were mainly present in the surfactant rich interfacial layers which led to the droplet size increases.

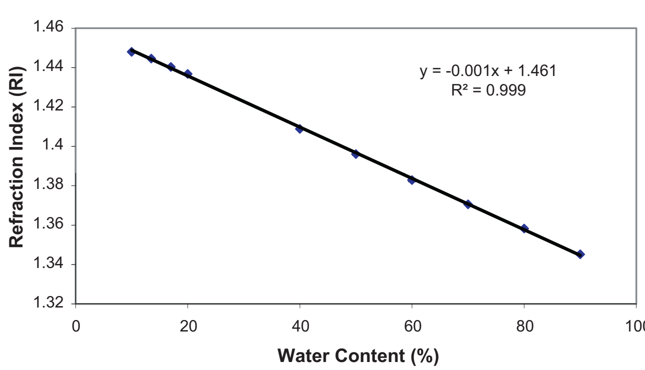

Fig. 2. The plot of refraction index (RI) vs. water content (Φ_W) plot with the linear regression for microemulsions along the water dilution line of O/(S/Co-S) ratio 1/9.

Table 2
Ketoprofen, lidocaine, and caffeine solubility in selected formulation excipients measured at the ambient temperature.

Excipient	Solubility (mg/mL)		
	Ketoprofen	Lidocaine	Caffeine
IPM	12.2	131.3	0.8
IPP	9.2	109.6	NT
Oleic acid	1.3	184.1	NT
Miglyol 812	10.0	NT	NT
Miglyol 840	16.8	NT	NT
Labrafac	16.1	NT	1.8
Labrasol	154.6	216.9	11.9
Cremophor EL	108.6	110.3	7.6
Ploural Oleique	28	99.0	1.7
PG	151.2	365.7	8.9
Water	0.2	3.7	19.9

Note: NT, not tested.

3.1.4. Electrical conductivity

The oil/surfactant mixture of O/(S/Co-S) ratio 1/9 was diluted by the aqueous phase, 0.9% (w/v) NaCl, gradually. EC values of MEs, κ, were measured in the dilution process and plotted vs. aqueous content Φ_W, as shown in Fig. 3. The κ vs. Φ_W curve could be divided into three parts: parts at low and high aqueous contents, and the part at median aqueous content. Based on previous studies (Mo et al., 2000; Alany et al., 2001;), at low aqueous content,

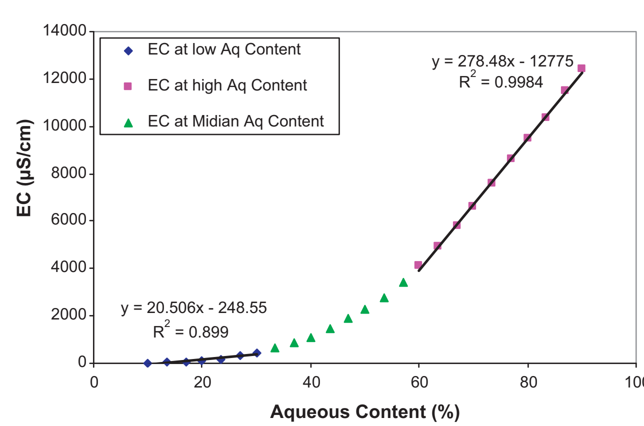

Fig. 3. The plot of microemulsion electrical conductivity κ vs. aqueous content Φ_W.

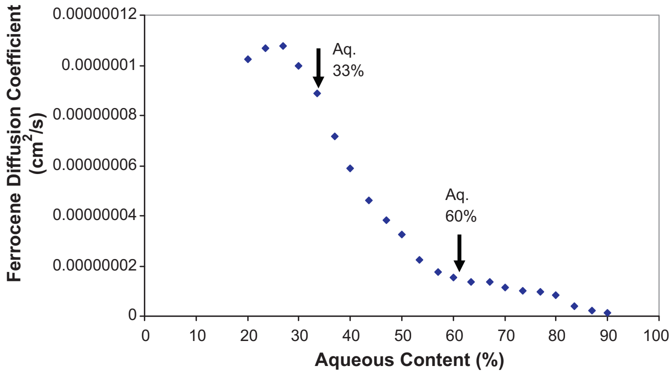

Fig. 4. The plot of apparent diffusion coefficient of ferrocene, *D* vs. aqueous content of microemulsions along the water dilution line of oil to surfactant ratio 1/9.

the microstructure is perceivably being as W/O. The electrical conductive entities will be the aqueous droplets that are in isolated state, resulting in the low conductivity at this region in which the curve of κ vs. Φ_W appeared to be linear. As the aqueous content Φ_W increases, the W/O droplets increase in number and start to aggregate, when the percolation point, Φ_p is reached, W/O droplets begin to contact each other and form inter-connected channels, resulting in a drastic increase of κ. Therefore, the turning point on the curve of κ vs. Φ_W from the linear to the non-linear increase is indicative of Φ_p and corresponds to the transformation from a W/O droplet to a Bi-continuous ME; At high aqueous content, the microstructure is O/W and the conductive entity is the continuous aqueous phase. As aqueous content Φ_W further increases, κ of the ME is expected to behave like an aqueous solution, increasing linearly. Again, the turning point on the plot of κ vs. Φ_W from the median aqueous non-linear region to the high aqueous linear region is indicative of the microstructure transformation from a Bi-continuous to an O/W ME; as showed in Fig. 3, κ vs. Φ_W curves at low and high Φ_W regions indeed can be approximated by linear fitting and yielded good correlation coefficients, respectively. The curve at the median Φ_W region is non-linear and therefore, should correspond to the Bi-continuous ME microstructure. Based on the EC results, it can be deduced microstructure transition points from W/O to Bi-continuous and from Bi-continuous to O/W are at water content of about 33% and 60%, respectively.

3.1.5. Electro-chemical method, cyclic voltammetry

The apparent diffusion coefficient, *D*, of the electro chemical active compound ferrocene was measured in ME samples resulting from the dilution of the oil/surfactant mixture of O/(S/Co-S) ratio 1/9 by the aqueous phase, 0.2 M KCl. The plot of *D* vs. aqueous content Φ_W is illustrated in Fig. 4. Similar to the dilution process in the EC measurement experiment, it was expected that the ME microstructure goes through transformation from W/O to Bi-continuous to O/W. Based on the previous reports (Mo et al., 2000; Mo and Li, 2007), ferrocene as a lipophilic compound will mainly dissolve in the oil phase, and is expected to have relatively high diffusion coefficient *D* values in W/O ME, relative low *D* values in O/W ME, and median *D* values in Bi-continuous ME. Therefore, based on the plot of ferrocene *D* vs. Φ_W, it can be deduced that microstructure transition points are at Φ_W of around 33% and 60% for changes from W/O to Bi-continuous and from Bi-continuous to O/W, respectively. These results are consistent with the observations in the EC experiment.

3.1.6. DSC thermal analyses

ME samples were tested using DSC for a cooling and heating cycle. After extensive sample tests, it was found that the cooling DSC thermo-gram provided direct information on ME sample microstructures. Specifically, it was discovered that there were some important characteristics of the cooling thermo-gram related to the oil freezing peak and the water freezing peak. They can be described as follows: (1) ME samples of W/O microstructure did not show the water freezing peak, (2) ME samples of Bi-continuous microstructure had the oil freezing peak and the water freezing peak as two distinct and separate peaks, and (3) ME samples of O/W microstructure showed only the water freezing peak as one big single peak in the thermo-gram. Based on these unique traits, the microstructure of a ME sample can be determined by a single DSC run. The DSC cooling thermo-grams of ME samples in microstructure transition regions are illustrated in Fig. 5. The microstructure transition points along the water dilution line of O/(S/Co-S) ratio 1/9 were easily determined to be at water content of 33% and 59% for microstructure changes from W/O to Bi-continuous and from Bi-continuous to O/W, respectively. These microstructure transition point results are consistent with results obtained earlier by EC and CV measurements. This above described DSC approach to determine ME microstructures by following the cooling thermo-gram characteristics has not been clearly identified and demonstrated in previous literature reports to our knowledge. It offers several advantages including a simple test, a small required sample size, and an effective and accurate microstructure determination for both blank and drug loaded MEs. ME formulations loaded with model drugs (ketoprofen 2.5%, lidocaine 2.5%, and caffeine 1.0%) were tested using DSC. The results confirmed that at

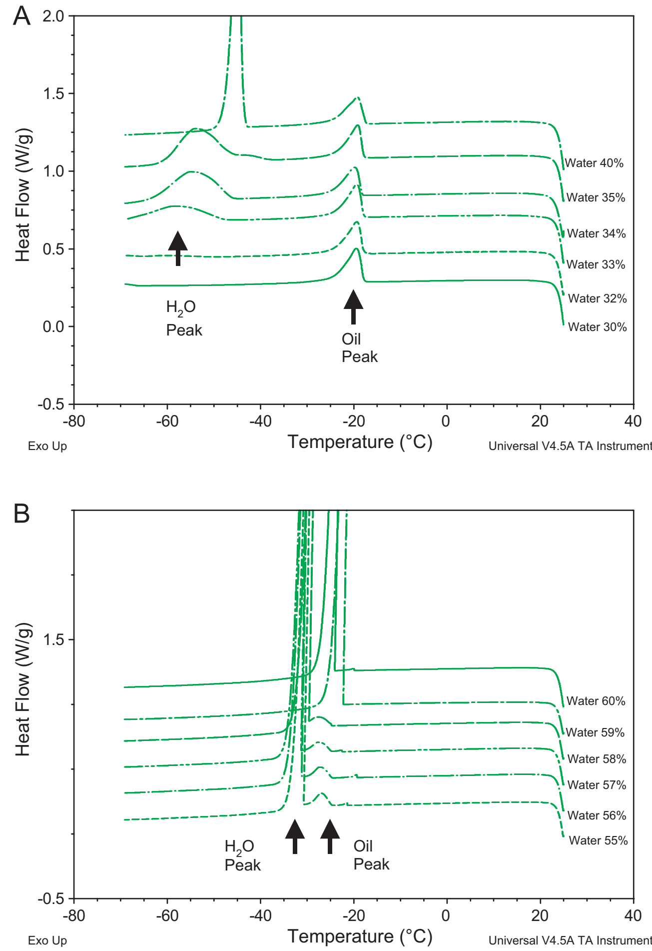

Fig. 5. DSC cooling thermo-grams of microemulsions at microstructure transition regions: (A) the transition from W/O to Bi-continuous ME, and (B) the transition from Bi-continuous to O/W ME.

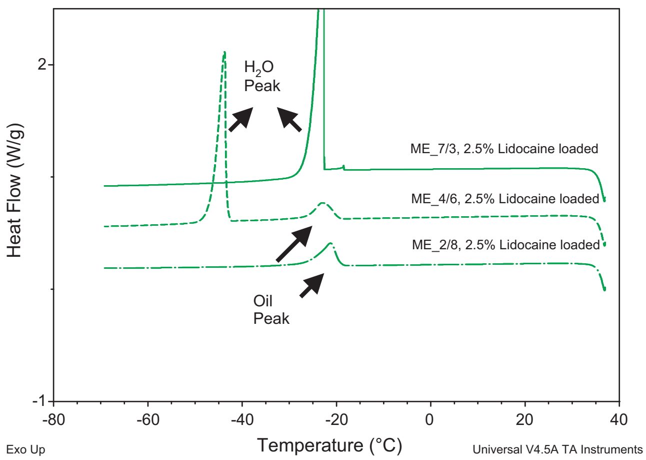

Fig. 6. DSC cooling thermo-grams of 2.5% lidocaine loaded MEs at 37 °C.

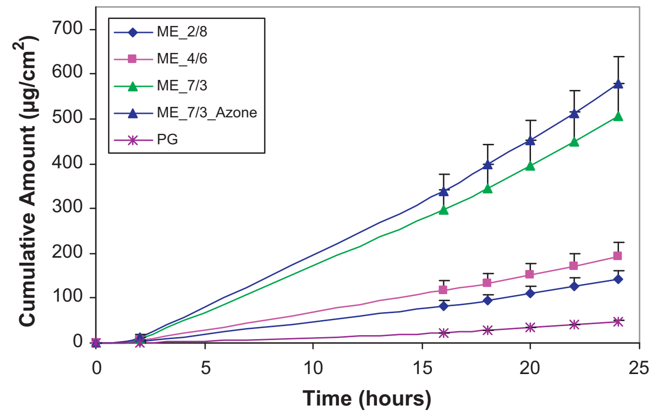

Fig. 8. Lidocaine cumulative permeation amount vs. time curves of microemulsion and the control formulations (data point + S.E.).

37 °C, these model drug loaded ME formulations were indeed in the microstructure of W/O, Bi-continuous, and O/W corresponding to water content of 20%, 40%, and 70%, respectively. Fig. 6 shows representative DSC cooling thermo-grams of 2.5% lidocaine loaded ME formulations.

3.2. Model drug solubility in microemulsion excipients

Model drugs, ketoprofen, lidocaine, and caffeine solubility samples in various excipients used in microemulsion and the control formulations were tested at the ambient temperature (25 °C) and the results are presented in Table 2.

3.3. Skin permeation results

The compositions and microstructures of the microemulsion vehicles used in skin permeation experiments are listed in Table 3, and their positions in the pseudo-ternary phase diagram are showed in Fig. 1.

Initially, drug loaded microemulsions prepared at the fixed oil to surfactant ratio 1/9 were studied for skin permeation. The results are summarized in Table 4, and illustrated in Figs. 7–9. PG is a known formulation vehicle to offer drug permeation enhancement (Williams and Barry, 2004) and was used as the control formulation. It is worth to note that PG vehicle sometimes could be a “negative control” when it possesses a lower thermothermodynamic activity for its loaded drug. However, it still serves as a reference in many studies because it is a perfect solvent for various drugs. For both lipophilic and hydrophilic drugs, microemulsions showed significantly higher or comparable permeation compared with the PG control formulation, therefore, ME formulations provided significant enhancement effects. Drug steady-state permeation flux, J_s, and cumulative permeation amount, $Q_{24\,h}$, increased significantly with water content in microemulsions. Since water content is related directly with microstructures, it can be derived that drug permeation is related to microemulsion microstructures, and at the fixed oil to surfactant ratio, the permeation increases in an order of microstructures as follows: W/O < Bi-continuous < O/W.

Fig. 7 and Table 4 showed that ketoprofen permeation fluxes from ME formulations increased significantly ($P<0.05$) with increased water content. Compared with the control, enhancement ratio, ER values were 1.86, 3.30, and 9.27 for ME water content of 20%, 40%, and 70%, corresponding to ME microstructure of W/O, Bi-continuous, and O/W, respectively. The permeation enhancer, Azone incorporated ME formulations (2%, w/w load) did not increase the permeation further; While the permeation enhancer, Br-IMSF incorporated ME formulation, ME_7/3_keto_Br-IMSF (2%, w/w load) showed to increase J_s further by about 25% compared with the ME formulation without the enhancer, however, the difference was not statistically significant ($P>0.05$).

Fig. 8 and Table 4 showed lidocaine skin permeation from ME and the control formulations. The results are similar to ketoprofen. For permeation enhancers incorporated ME formulations, at water content of 70%, Azone containing ME provided 13% higher J_s compared to the ME without Azone. At water content of 40%, Azone or Br-IMSF containing MEs resulted in J_s further increases of 34%

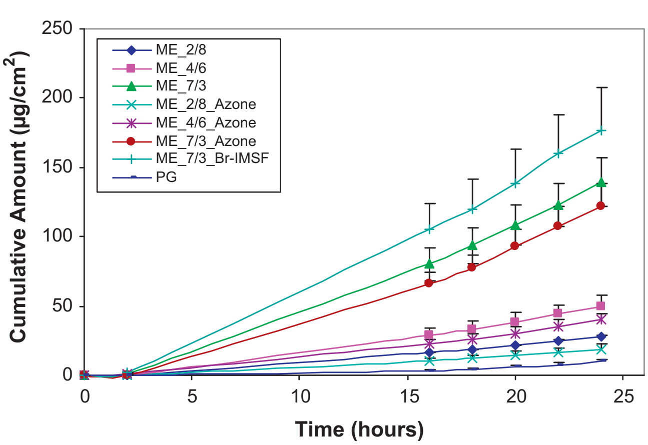

Fig. 7. Ketoprofen cumulative permeation amount vs. time curves of microemulsion and the control formulations (data point + standard error (S.E.)).

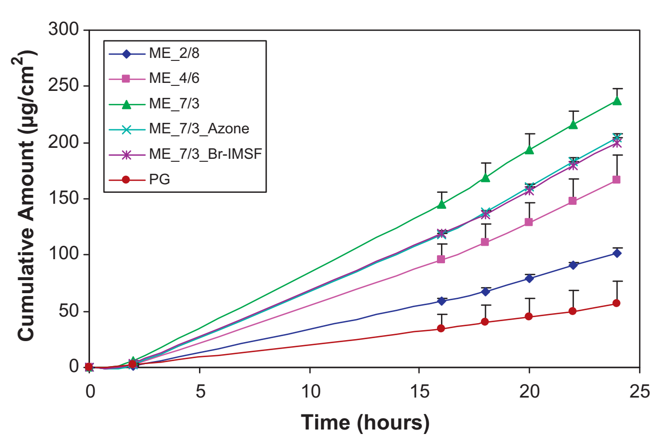

Fig. 9. Caffeine cumulative permeation amount vs. time curves of microemulsion and the control formulations (data point + S.E.).

Table 3
Microemulsion vehicle compositions and microstructures.

ME or Micelle Label	Position in phase diagram	Water to oil/surfactant ratio	Water (%)	Oil (%)	S/CoS (%)	O/(S/CoS) ratio	Microstructure
ME_2/8	A	20/80	20	8	72	1/9	W/O
ME_4/6	B	40/60	40	6	54	1/9	Bi-continuous
ME_7/3	C	70/30	70	3	27	1/9	O/W
ME_8/2	D	80/20	80	2	18	1/9	O/W
ME_5/5	E	50/50	50	5	45	1/9	Bi-continuous
ME_2/8_O	F	20/80	20	16	64	2/8	W/O
ME_3/7_O	G	30/70	30	14	56	2/8	Bi-continuous
ME_4/6_O	H	40/60	40	12	48	2/8	Bi-continuous
ME_5/5_O	I	50/50	50	10	40	2/8	Bi-continuous
Micelle_5/5	J	50/50	50	0	50	0/10	NT
Micelle_7/3	K	70/30	70	0	30	0/10	NT

Note: NT, not tested; S, surfactant; CoS, co-surfactant.
ME labeled as "ME_water/(oil/surfactant) ratio" contains oil/surfactant mixture of the ratio 1/9.
ME labeled as "ME_water/(oil/surfactant) ratio_O" contains oil/surfactant mixture of the ratio 2/8.

and 16%, respectively. However, the differences observed between MEs with and without enhancers were not statistically significant ($P > 0.05$).

Fig. 9 and Table 4 showed the permeation of hydrophilic caffeine also increased with water content significantly ($P < 0.05$); at water content of 70%, ME formulations with enhancers, Azone or Br-IMSF incorporated resulted in slightly lower but not statistically significant different permeation compared with MEs without enhancers.

Fig. 10 shows ER vs. water content plot for all three model drugs. As water content increased, for lipophilic drug ketoprofen and lidocaine, ER increased in a more pronounced manner, and seemed to follow an exponential growth trend, while for hydrophilic caffeine, ER appeared to increase linearly.

Further ketoprofen permeation experiments were conducted using ME formulations at oil to surfactant ratios of 1/9 and 2/8, and micelle formulations without oil, to investigate the influence of oil content on skin permeation. The results are illustrated in Table 5 and Fig. 11. At the same water content of 50%, ketoprofen permeation J_s increased significantly ($P < 0.05$) as oil content increased from 0% to 10%. The results suggest that at the same water content, ketoprofen permeation increases with oil content in the formulation, and micellar formulation (contains no oil) provided the lowest permeation flux. Fig. 11(A) shows ER values from ME formulations with oil to surfactant ratio of 2/8 are higher than those from ME formulations with oil to surfactant ratio of 1/9 when compared at the same water content, again indicating that increasing oil content will lead to an increase in ketoprofen permeation. Skin permeation results generally bear high variability partly due to skin sample variation among individual animal donors, the ER comparisons based on data from skin of different animals provide a normalized evaluation of the drug permeation and decreased variability from permeation flux data of different animal donors to certain extent.

Fig. 11(B) shows non-linear exponential fitting of ER vs. water content curves of ME formulations with oil to surfactant ratio of 1/9 and 2/8. Good correlation coefficients (R^2) were obtained, 0.9886 and 0.9968 for MEs of O/S 1/9 and 2/8, respectively. The results demonstrate that the ER of ketoprofen correlates with and appears to increase with water content in an exponential fashion.

Table 4
Skin steady-state permeation fluxes, J_s (mean ± S.D.) and cumulative permeated amounts, $Q_{24\,h}$ (mean ± S.D.) of model drugs from microemulsions and the control formulations.

Formulation (vehicle_drug_enhancer)	Water (w/w %)	J_s (μg/cm^2/h)	ER	$Q_{24\,h}$ (μg/cm^2)
ME_2/8_Keto[a]	20	1.49 ± 0.12	1.86	27.96 ± 1.79
ME_4/6_Keto[a]	40	2.64 ± 0.69	3.30	50.04 ± 15.81
ME_7/3_Keto[a]	70	7.41 ± 1.46	9.27	139.57 ± 34.39
ME_2/8_Keto_Azone[a]	20	1.06 ± 0.45	1.33	18.78 ± 6.74
ME_4/6_Keto_Azone[a]	40	2.19 ± 0.35	2.74	39.95 ± 8.57
ME_7/3_Keto_Azone[a]	70	7.05 ± 1.97	8.82	121.43 ± 29.32
ME_7/3_Keto_Br-IMSF[a]	70	9.23 ± 2.62	11.55	177.15 ± 53.04
PG_Keto[a]	0	0.80 ± 0.29	1.00	9.82 ± 3.28
ME_2/8_Lido[a]	20	7.50 ± 2.17	2.37	142.83 ± 35.94
ME_4/6_Lido[a]	40	9.66 ± 2.36	3.06	194.30 ± 53.94
ME_7/3_Lido[a]	70	26.28 ± 5.66	8.32	505.91 ± 111.87
ME_2/8_Lido_Azone[a]	20	5.98 ± 1.75	1.89	125.22 ± 41.26
ME_4/6_Lido_Azone[a]	40	12.95 ± 1.57	4.10	255.16 ± 26.14
ME_4/6_Lido_Br-IMSF[a]	40	11.23 ± 2.95	3.55	238.18 ± 46.69
ME_7/3_Lido_Azone[a]	70	29.78 ± 4.28	9.42	579.30 ± 88.87
PG_Lido[a]	0	3.16 ± 0.18	1.00	47.78 ± 3.25
ME_2/8_Caff[a]	20	5.44 ± 0.33	1.97	102.07 ± 5.75
ME_4/6_Caff[a]	40	8.86 ± 1.95	3.21	166.63 ± 35.70
ME_7/3_Caff[a]	70	11.63 ± 0.72	4.21	237.79 ± 25.49
ME_2/8_Caff_Azone[a]	20	5.11 ± 1.11	1.85	91.79 ± 16.86
ME_7/3_Caff_Azone[a]	70	10.82 ± 0.76	3.92	204.50 ± 6.86
ME_7/3_Caff_Br-IMSF[a]	70	10.16 ± 0.64	3.68	199.72 ± 7.36
PG_Caff[a]	0	2.76 ± 1.46	1.00	56.32 ± 31.54

Note: ketoprofen, lidocaine, and caffeine log P: 3.2, 2.1, and −0.5 (from DrugBank).
For each tested formulation, $n = 3$–5.
ER: enhancement ratio for drug permeation = J_s in microemulsion/J_s in PG.
[a] Significant difference observed among ME formulations with different water contents and the control formulation, $P < 0.05$.

Table 5
Ketoprofen permeation steady-state flux, J_s (mean ± S.D.) and cumulative permeation amount, $Q_{24\,h}$ (mean ± S.D.) from microemulsion and micelle formulations.

Formulation (vehicle_drug)	Water (w/w %)	O/S	J_s (μg/cm²/h)	ER	$Q_{24\,h}$ (μg/cm²)
ME_5/5_Keto[a,b,c]	50	1/9	5.29 ± 0.30	7.25	109.84 ± 8.43
ME_5/5_O_Keto[a,b,c]	50	2/8	7.67 ± 1.55	10.51	152.22 ± 37.28
ME_7/3_Keto[a,b,c]	70	1/9	9.92 ± 2.25	13.59	190.37 ± 45.80
ME_8/2_Keto[a,c]	80	1/9	12.92 ± 2.03	17.70	261.60 ± 47.07
Micelle_5/5_Keto[a,b,c]	50	0/10	1.21 ± 0.36	1.66	27.08 ± 6.31
Micelle_7/3_Keto[a,b,c]	70	0/10	3.95 ± 0.96	5.41	69.18 ± 44.82
PG_Keto[a,c]	0	NA	0.73 ± 0.16	1.00	9.07 ± 2.43
ME_2/8_O_Keto[a,d]	20	2/8	0.34 ± 0.05	2.13	5.35 ± 0.30
ME_3/7_O_Keto[a,d]	30	2/8	0.59 ± 0.24	3.69	10.37 ± 4.44
ME_4/6_O_Keto[a,c,d]	40	2/8	0.88 ± 0.12	5.50	14.67 ± 2.24
ME_5/5_O_Keto[a,d]	50	2/8	1.59 ± 0.41	9.94	25.08 ± 6.78
PG_Keto[a,d]	0	NA	0.16 ± 0.17	1.00	1.95 ± 2.20

Note: NA, not applicable.
For each tested formulation, n = 3–5.
O/S: oil to surfactant (and co-surfactant) ratio.
[a] Significant difference observed among ME formulations with different water contents and the control formulation, $P < 0.05$.
[b] Significant difference observed among ME and micelle formulations with different oil content, $P < 0.05$.
[c] Permeation experiments were conducted using porcine skins from different animals.
[d] Permeation experiments were conducted using porcine skins from the same animal.

Table 6
Ketoprofen permeation steady-state flux, J_s (mean ± S.D.) and cumulative permeation amount, $Q_{24\,h}$ (mean ± S.D.) from microemulsion formulations containing different oil components.

Formulation (vehicle_oil_%content)	Water (w/w %)	Oil name	Oil (w/w %)	J_s (μg/cm²/h)	$Q_{24\,h}$ (μg/cm²)
ME_5/5_IPM_5%[a]	50	IPM	5	2.89 ± 0.56	53.17 ± 10.76
ME_5/5_IPM_10%[a]	50	IPM	10	3.97 ± 0.14	76.01 ± 7.32
ME_5/5_OA_5%[a]	50	OA	5	2.34 ± 0.96	43.82 ± 15.91
ME_5/5_ML812_5%[a]	50	ML840	5	1.57 ± 0.45	30.05 ± 8.64
ME_5/5_ML840_5%[a]	50	ML812	5	1.96 ± 0.63	35.37 ± 10.36

Note: OA, oleic acid; ML840, Miglyol 840; ML812, Miglyol812.
For various formulations, n = 3–4.
[a] Significant difference observed among ME formulations with different oils or oil contents, $P < 0.05$.

Additional ketoprofen permeation experiments were conducted using microemulsions with different oils in formulations in order to investigate oil component effects on drug permeation. The results are tabulated in Table 6. At the same water content of 50%, ketoprofen permeation flux was significantly higher ($P < 0.05$) when oil (IPM) content increased from 5% to 10%, this was a reproducible result compared with the same experiment in Table 5, although permeation flux data varied due to differences in porcine skin from different animals. Permeation fluxes were also affected by different oils but at the same concentration in formulations. In an increasing order of ketoprofen permeation flux, oils can be ranked as follow:

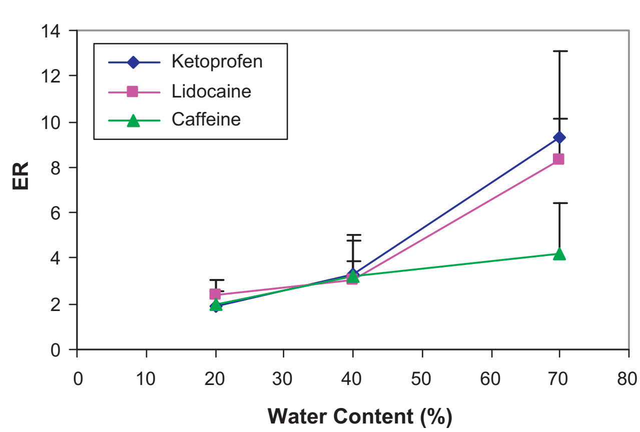

Fig. 10. Enhancement ratio, ER from microemulsion formulations vs. water content plots for three model drugs, ketoprofen, lidocaine and caffeine (data showing ER + S.D.)..

Miglyol 812 < Miglyol 840 < oleic acid < IPM. These results suggest that different oils used in ME formulations will have some effect on the drug permeation. However, the permeation J_s did not show a correlation with the drug solubility in these oils (Table 2).

4. Discussion

Refraction index of MEs vs. water content plot showed a good linear correlation ($R^2 = 0.9996$). The linear relationship between RI and water content reflects the optically isotropic characteristic of ME, which had not been reported before to our knowledge. The linear range of RI vs. water content of MEs can be used to verify the range of ME along the certain water dilution line, and also possibly for ME sample stability monitoring.

Electrical conductivity measurement is the most commonly used method for ME microstructure characterizations. In most previous studies (Djordjevic et al., 2004; Podlogar et al., 2004, 2005; Lopes et al., 2010), EC tests were conducted for assessing the phase change of ME samples by gradual dilution using pure water as the aqueous phase. However, this method was often not obvious and effective to determine microstructure changes in many cases of ME systems of non-ionic surfactants, because of low EC value and no clear turning points to follow in the curve slopes. In this study, a low concentration NaCl salt (0.9%, w/v) solution was used as the aqueous phase for the dilution. The resulting EC vs. water content curve showed the three distinct parts, which could be fitted by linear regressions at low and high aqueous phase regions, corresponding to W/O and O/W microstructures. Using this approach, microstructure transition points can be estimated easily and directly. For ME systems of non-ionic surfactants, a low concentration salt solution employed for the dilution was found not to change the ME

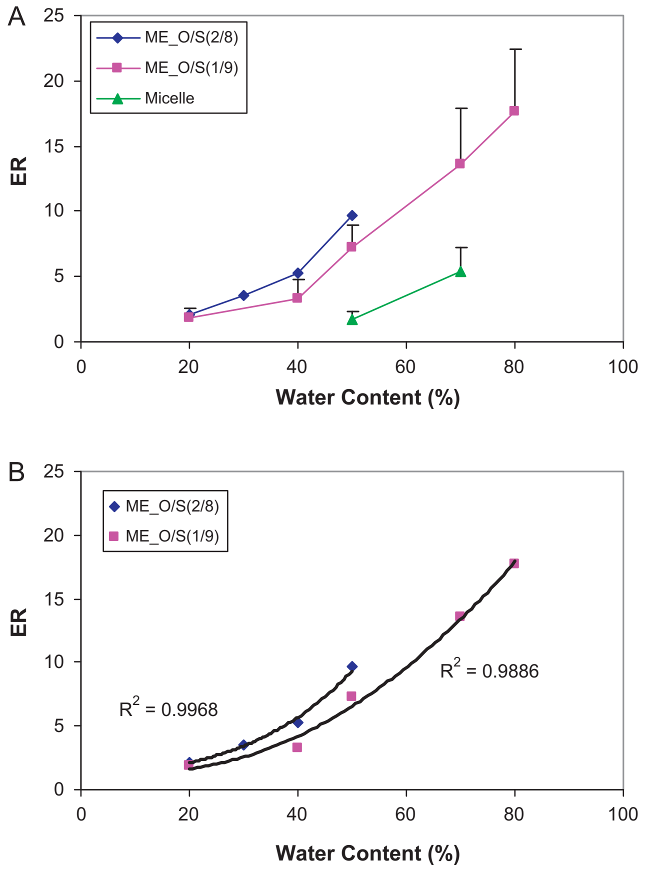

Fig. 11. (A) ER vs. water content plots for ketoprofen ME and micelle formulations, and (B) non-linear exponential fitting to ER vs. water content curves.

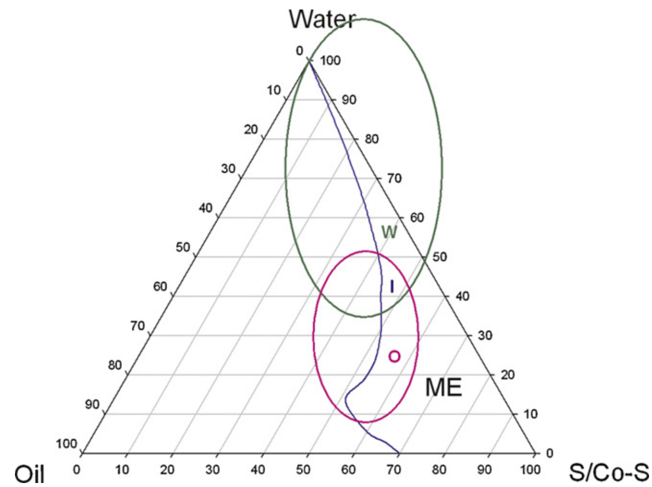

Fig. 12. Microemulsion pseudo-ternary phase diagram with labeled regions of high water content, W, high oil content, O, and balanced water and oil content, I.

phase behavior significantly. This observation was consistent with the previous reports (Alany et al., 2001; Chaiyana et al., 2010)

The CV method to test ME microstructure has only few reports (Mo et al., 2000; Mo and Li, 2007) in the area of electro-chemical study, and has not been applied to ME formulations related to drug delivery. In this study, the results showed that the CV method was an effective approach for deriving microstructure information of ME formulations for drug delivery, and provided complemented results to those from other methods.

Progress has been made in this study when using the DSC technique for ME microstructure characterization. In the previously published studies (Podlogar et al., 2004, 2005; Boonme et al., 2006; Liu et al., 2009), DSC had been used for the same purpose, but the unique characteristics of the cooling thermo-gram of ME samples that led to the ME phase information was not clearly identified. We probably can explain the phenomena observed in this study by visualizing interactions at a molecular level between different phase components. In W/O MEs, water was dispersed molecularly and bound tightly with surfactants, it could not be frozen, so no water freezing peak was observed. As water content increased in Bi-continuous MEs, there free water started to be present causing water droplet significant elongation and furthermore the formation of water cylinder or channel structures, therefore, the freezing peak of free bulk water was observed. In O/W MEs, it was either because oil molecules disperse and interact strongly with surfactants and could not be frozen or because water and oil freezing peaks overlaid due to the water peak moving to higher temperature, only one large water freezing peak was observed. Therefore, DSC cooling thermo-grams reveals direct information of molecular interactions of ME phase components and of microstructures.

Drug permeation increases with water content of ME systems has been reported by Sintov and Shapiro (2004). However, in the particular study, the ME system could only solubilize up to 30% water, which prevented the author to draw conclusions regarding drug permeation relationship to different microstructures, which only exist and evolve in a wide range of water content. Podlogar's group (2005) studied ketoprofen release from MEs of different water contents, and showed the release rate J_S increased with water content and attributed the phenomena to increased ketoprofen diffusion inside formulations with higher water content. However, over the same range of water content change, the extent of increase of ketoprofen release rate was much less than that of increase of ketoprofen transdermal permeation flux observed in the current study. Therefore, ketoprofen diffusion maybe part of, but not all the cause for the observed transdermal permeation enhancement. For lipophilic drug ketoprofen and lidocaine, the relationship of permeation enhancement with water content can still be explained by the mechanism of increasing drug thermodynamic activity in MEs that have high water contents.

Water content and oil content were identified to be two principal factors that affect drug transdermal permeation potential in this study. That is to say increasing water content, or oil content at the fixed water content, or both will lead to the increase of drug permeation. By reviewing literature on microemulsions for transdermal drug delivery, it was found that most previous reports are consistent with the two principal factors. Some of the drugs in these reports include both lipophilic and hydrophilic ones: lidocaine, prilocaine hydrochloride, vinpocetine, cyclosporin A, tolterodine, testosterone, ketoprofen, ibuprofen, indomethacin, buspirone hydrochloride, theophylline, lacidipine, capsaicin derivative, and triptolide (Kreilgaard et al., 2000; Sintov and Shapiro, 2004; Hua et al., 2004; Liu et al., 2009; Elshafeey et al., 2009; Hathout et al., 2010; Rhee et al., 2001; Chen et al., 2006; Maghraby, 2010; Tsai et al., 2011; Zhao et al., 2006; Gannu et al., 2010; Huang et al., 2008; Chen et al., 2004). Based on observations in the current study and literature reports, we propose an optimal ME formulation region concept in the pseudo-ternary phase diagram. Fig. 12 illustrated the concept which showing different ME regions in the pseudo-ternary phase diagram. The ME formulation composition of high trandermal drug permeation potential should fall into the regions of high water content (Region W), or the region of balanced water and oil content but low surfactant content (Region I). It is interesting to note that in the literature reports, most of the optimal ME formulations were indeed from Region W, and some of the optimal ME formulations were from Region I (Rhee et al., 2001; Chen et al., 2004; Liu et al., 2009).

There are some reports that are not consistent with our proposed optimal ME region concept of high water content, balanced oil content and low surfactant content. These reports (Baroli et al., 2000; Peltola et al., 2003; Yuan et al., 2006; Zhu et al., 2008) had the optimal ME formulations containing relatively high surfactant mixture contents. In all these cases, the ME systems under investigations used short chain alcohol such as ethanol as the co-surfactant. Because ethanol is a well-known permeation enhancer itself (Gao and Singh, 1998), higher surfactant mixture content increased the ME formulation permeation potential. Therefore, we can view the ME systems using ethanol as co-surfactant are exceptional to the above proposed optimal ME formulation region concept.

Although we report water content and oil content are the two key factors affecting drug transdermal permeation enhancement, which are the focus of this study, there are other factors that also play a role in controlling drug permeation, for example, the surfactant to co-surfactant (S/Co-S) ratio (Kreilgaard et al., 2000; Sintov and Shapiro, 2004; Hua et al., 2004; Rhee et al., 2001; Maghraby, 2008; Huang et al., 2008). In ME formulation development, it is necessary to optimize S/Co-S ratios, which were shown to be unique for the different ME systems. Additionally, it was shown that different oils used in ME will have some effect on drug transdermal permeation in the study in which IPM, oleic acid, Miglyol 812, and Miglyol 840 were tested.

5. Conclusion

Microemulsion formulations showed significant transdermal permeation enhancement effect for lipophilic and hydrophilic model drugs, ketoprofen, lidocaine, and caffeine. The two key factors that strongly influenced drug transdermal permeation potential from ME formulations were water content and oil content. Drug permeation increased with water content, for lipophilic drugs, permeation appeared to increase in an exponential manner while for hydrophilic drugs, permeation appeared to increase linearly. Transdermal drug delivery potential is also related to ME microstructures, along a given water dilution line, in an increasing order of drug permeation it was identified: W/O < Bi-continuous < O/W. At the same water content, increasing oil content will lead to higher drug permeation. The above observations provide practical guidance to ME transdermal formulation development. ME formulations with permeation enhancer, Azone or Bromo-imnosulfurane incorporated in general did show significant further permeation enhancement effect in the study. Characterizations of ME microstructure is important for gaining insight into permeation enhancement mechanisms and for developing ME formulations. This was achieved by successful utilization of a combination of testing techniques, e.g. DSC, CV, EC and DLS. The DSC technique was further developed in the study, which allowed an easy and accurate determination of ME microstructures.

The results from the present study may pave the way for future pharmaceutical work. Further studies should include more drugs of various physicochemical properties, such as different molecular masses, polarities, solubilities. The mechanism of drug permeation via microemulsion systems can also be evaluated by alteration and learning of their microstructure. It is also important to investigate MEs for easy skin administration, e.g. to prepare them as gel or patch formulations while maintaining high drug permeation capability. The studies in this area will provide information useful for ME applications in transdermal drug delivery for various treatments, e.g. pain relief, hormone replacement, anti-depression, and eventually offer benefits to patients.

Acknowledgements

This paper is based on a part of Ji Zhang's graduate research for a Ph.D. degree. The authors would like to acknowledge the support of an education assistantship from Merck & Co. during the period of the study, Dr. Sintov Amnon for kind help on giving comments on the manuscript, and Gattefosse for the gift of lipid samples. In addition, the authors would like to express their gratitude to the New Jersey Center for Biomaterials for access to equipment.

References

Alany, R.G., Tucker, I.G., Davies, N.M., Rades, T., 2001. Characterizing colloidal structures of pseudoternary phase diagrams formed by oil/water/amphiphile systems. Drug Dev. Ind. Pharm. 27, 31–38.

Azeem, A., Khan, Z.I., Aqil, M., Ahmad, F.J., Khar, R.K., Talegaonkar, S., 2009. Microemulsion as a surrogate carrier for dermal drug delivery. Drug Dev. Ind. Pharm. 35, 525–547.

Baroli, B., Lopez-Quintela, M.A., Delgado-Charro, M.B., Fadda, A.M., Blanco-Mendez, J., 2000. Microemulsion for topic delivery of 8-methoxsalen. J. Control. Release 69, 209–218.

Boonme, P., Krauel, K., Graf, A., Rades, T., Junyaprascert, V.B., 2006. Characterization of microemulsion structures in the pseudoternary phase diagram of isopropyl palmitate/water/Brij 97:1-butanol. AAPS PharmSciTech 7, E1–E6.

Chaiyana, W., Saeio, K., Hennink, W.E., Okonogi, S., 2010. Characterization of potent anticholinesterase plant oil based microemulsion. Int. J. Pharm. 401, 32–40.

Chen, H., Chang, X., Weng, T., Zhao, X., Gao, Z., Yang, Y., Xu, H., Yang, X., 2004. A study of microemulsion systems for transdermal delivery of triptolide. J. Control. Release 98, 427–436.

Chen, H., Chang, X., Du, D., Li, J., Xu, H., Yang, X., 2006. Microemulsion-based hydrogel formulation of ibuprofen for topical delivery. Int. J. Pharm. 315, 52–58.

Djordjevic, L., Primorac, M., Stupar, M., Krajisnik, D., 2004. Characterization of caprylocaproyl macrogoglycerides based microemulsion drug delivery vehicles for an amphiphilic drug. Int. J. Pharm. 271, 11–19.

Djordjevic, L., Primorac, M., Stupar, M., 2005. In vitro release of diclofenac diethylamine from caprylocaproyl macrogoglycerides based microemulsions. Int. J. Pharm. 296, 73–79.

Dong, X., Ke, X., Liao, Z., 2011. The microstructure characterization of meloxicam microemulsion and its influence on the solubility capacity. Drug Dev. Ind. Pharm. 37, 894–900.

Elshafeey, A.H., Kamel, A.O., Fathallal, M.M., 2009. Utility of nanosized microemulsion for transdermal delivery of tolterodine tartrate: ex-vivo permeation and in-vivo pharmacokinetic studies. Pharm. Res. 11, 2446–2453.

El Maghraby, G.M., 2008. Transdermal delivery of hydrocortisone from eucalyptus oil microemulsion: effects of cosurfactants. Int. J. Pharm. 355, 285–292.

El Maghraby, G.M., 2010. Self-microemulsifying and microemulsion systems for transdermal delivery of indomethacin: effect of phase transition. Colloid Surf. B: Biointerfaces 75, 595–600.

Gannu, R., Palem, C.R., Yamsani, V.V., Yamsani, S.K., Yamsani, M.R., 2010. Enhanced bioavailability of lacidipine via microemulsion based transdermal gels: formulation optimization, ex vivo and in vivo characterization. Int. J. Pharm. 388, 231–241.

Gao, S., Singh, J., 1998. Effect of oleic acid/ethanol and oleic acid/propylene glycol on the in vitro percutaneous absorption of 5-fluorouracil and tamoxifen and the macroscopic barrier property of porcine epidermis. Int. J. Pharm. 156, 45–55.

Hathout, R.M., Woodman, T.J., Mansour, S., Mortada, N.D., Geneidi, A.S., Guy, R.H., 2010. Eur. J. Pharm. Sci. 40, 188–196.

Heuschkel, S., Goebel, A., Neubert, R.H.H., 2008. Microemulsions—moderncolloidal carrier for dermal and transdermal drug delivery. J. Pharm. Sci. 97, 603–631.

Hua, L., Weisan, P., Jiayu, L., Ying, Z., 2004. Preparation evaluation, and NMR characterization of vinpocetine microemulsion for transdermal delivery. Drug Dev. Ind. Pharm. 30, 657–666.

Huang, Y.B., Lin, Y.H., Lu, T.M., Wang, R.J., Tsai, Y.H., Wu, P.C., 2008. Transdermal delivery of capsaicin derivative-sodium nonivamide acetate using microemulsions as vehicles. Int. J. Pharm. 349, 206–211.

Kreilgaard, M., Pedersen, E.J., Jaroszewski, J.W., 2000. NMR characterization and transdermal drug delivery potential of microemulsion systems. J. Control. Release 69, 421–433.

Kreilgaard, M., 2002. Influence of microemulsions on cutaneous drug delivery. Adv. Drug Delivery Rev. 54, s77–s98.

Lee, P.J., Langer, R., Shastri, V.P., 2003. Novel microemulsion enhancer formulation for simultaneously delivery of hydrophilic and hydrophobic drugs. Pharm. Res. 20, 264–269.

Liu, H., Wang, Y., Lang, Y., Yao, H., Dong, Y., Li, S., 2009. Bicontinuous cyclosporine A loaded water-AOT/Tween 85-isopropylmyristate microemulsions: structural characterization and dermal pharmacokinetics in vivo. J. Pharm. Sci. 98, 1167–1176.

Lopes, L.B., Vandewall, H., Li, H.T., Venugopal, V., Li, H.K., Naydin, S., Hosmer, J., Levendusky, M., Zheng, H., Bentley, M.V.L.B., Levin, R., Hass, M.A., 2010. Topical delivery of lycopene using microemulsions: enhanced skin penetration and tissue antioxidant activity. J. Pharm. Sci. 99, 1346–1357.

Mo, C., Zhong, M., Zhong, Q., 2000. Investigation of structure and structural transition in microemulsion systems of sodium dodecyl sulfonate + n-heptane + n-butanol + water by cyclic voltammetric and electrical conductivity measurements. J. Electroanal. Chem. 493, 100–107.
Mo, C., Li, X., 2007. Microstructure and structural transition in coconut oil microemulsion using semidifferential electroanalysis. J. Colloid Interface Sci. 312, 355–362.
Neubert, R.H.H., 2011. Potential of new nacocarriers for dermal and transdermal drug delivery. Eur. J. Pharm. Biopharm. 77, 1–2.
Peltola, S., Saarinen-Savolainen, P., Kiesvaara, J., Suhonen, T.M., Urtti, A., 2003. Microemulsions for topical delivery of estradiol. Int. J. Pharm. 254, 99–107.
Podlogar, F., Gasperlin, M., Tomsic, M., Jamnik, A., Rogac, M.B., 2004. Structural characterization of water-Tween 40/Imwiter 308 – isopropyl myristate microemulsions using different experimental methods. Int. J. Pharm. 276, 115–128.
Podlogar, F., Rogac, M.B., Gasperlin, M., 2005. The effect of internal structure of selected water-Tween 40 – Imwitor 308 – IPM microemulsions on ketoprofen release. Int. J. Pharm. 302, 68–77.
Rhee, Y.S., Choi, J.G., Park, E.S., Chi, S.C., 2001. Transdermal delivery of ketoprofen using microemulsions. Int. J. Pharm. 228, 161–170.
Sintov, A.C., Shapiro, L., 2004. New microemulsion vehicle facilitates percutaneous penetration in vitro and cutaneous drug bioavailability in vivo. J. Control. Release 95, 173–183.
Sintov, A.C., Botner, S., 2006. Transdermal drug delivery using microemulsion and aqueous systems: influence of skin storage conditions on the in vitro permeability of diclofenac from aqueous vehicle systems. Int. J. Pharm. 311, 55–62.
Sintov, A.C., Brandys-Sitton, R., 2006. Facilitated skin penetration of lidocaine: combination of a short-term iontophoresis and microemulsion formulation. Int. J. Pharm. 316, 58–67.
Song, Y., Xiao, C., Mendelsohn, R., Zheng, T., Strekowski, L., Michniak, B., 2005. Investigation of iminosulfuranes as novel transdermal penetration enhancers: enhancement activity and cytotoxicity. Pharm. Res. 22, 1918–1925.
Tsai, Y.H., Chang, J.T., Chang, J.S., Huang, C.T., Huang, Y.B., Wu, P.C., 2011. The effect of component of microemulsions on transdermal delivery of buspirone hydrochloride. J. Pharm. Sci. 100, 2358–2365.
Williams, A.C., Barry, B., 2004. Permeation enhancers. Adv. Drug Delivery Rev. 56, 503–618.
Yuan, Y., Li, S., Mo, F., Zhong, D., 2006. Investigation of microemulsion system for transdermal delivery of meloxicam. Int. J. Pharm. 321, 117–123.
Zhao, X., Liu, J.P., Zhang, X., Li, Y., 2006. Enhancement of transdermal delivery of theophylline using microemulsion. Int. J. Pharm. 327, 58–64.
Zhu, W., Yu, A., Wang, W., Dong, R., Wu, J., Zhai, G., 2008. Formulation design of microemulsion for dermal delivery of penciclovir. Int. J. Pharm. 360, 184–190.